Multiple-Scale Terrain Forcing of Local Wind Fields

J. C. DORAN AND E. D. SKYLLINGSTAD

Pacific Northwest Laboratory, Richland, Washington

(Manuscript received 15 April 1991, in final form 26 August 1991)

ABSTRACT

Observations and numerical simulations with a hydrostatic model are used to examine effects of regional and local terrain, synoptic forcing, and stability on the wind fields of an intermountain basin. The study area is centered on the Hanford site in southeast Washington. Two wintertime case studies are presented, each characterized by a surface inversion but with different synoptic forcing. In both cases, the local topography produces a region of blocked flow and significant horizontal wind shear, but slight differences in the direction of the synoptic winds lead to marked differences in the subsequent development of the wind fields over the site. Numerical experiments show that these differences are related to flow through gaps in the Cascade Mountains over 100 km to the west. Additional experiments show that a modest increase in vertical wind shear can cause significant alterations in the local flow patterns, the elimination of the blocked-flow region, and less sensitivity to regional or local terrain effects. Increased solar insolation also weakens the blocking effect of local terrain, but the effects of the Cascade Mountains can still be discerned.

1. Introduction

Terrain forcing is often an important factor in establishing mesoscale circulation patterns. For simplified topographical features with scales on the order of 100 km or more, there is now a good understanding of many aspects of leeside flow (e.g., Durran 1990). The flow patterns arising from forcing on these scales are often repetitive and somewhat predictable. For more complicated and realistic topography, however, the situation is less clear. Terrain forcing can then occur over a range of scales, and the details of the circulations may depend on all of them. Under such circumstances, it can be difficult to isolate the dominant forcing mechanisms responsible for a particular flow pattern or to characterize succinctly how such patterns respond to changes in the forcing. For example, the effects of relatively small differences in larger-scale flow patterns may be amplified by local topographic effects; conversely, local terrain features may lessen the impact of substantial changes in large-scale patterns. This poses a significant problem in terms of forecasting, numerical simulations, and data-assimilation techniques. Moreover, analytical simplifications that might make the problem more tractable are frequently inappropriate.

In the Pacific Northwest, terrain has a particularly large influence on mesoscale circulations. The dominant topographical feature of the area is the Cascade Mountains. The winter climatology of the region is characterized by alternating periods of strong westerly flow and stable, high pressure ridge patterns. When westerly flow is prevalent, weather on the west side of the Cascades is dominated by a moist marine air mass. On the east side of the mountains, this flow often produces a warm downslope condition with moderate surface winds. In contrast, the high pressure pattern leads to stable conditions on both sides of the Cascades, with the eastside intermountain basins becoming particularly stagnant. As a ridge pattern breaks down, the eastside basins can remain stagnant even though the winds aloft may be fairly strong. For example, winds at 1000 m are often as high as 15 m s^{-1} while the surface winds in the Columbia Basin are calm.

We were interested in the daytime evolution of the wind fields in basins during the winter, when surface-based inversions can persist through much of the day. The region selected for our study is a portion of the Columbia Basin in south-central Washington. We will show that in the presence of an inversion, the flow patterns in our study area are often relatively consistent for a range of synoptic wind directions. However, numerical simulations with a mesoscale model show that the local wind patterns may also exhibit pronounced sensitivity to the synoptic winds and a combination of local- and regional-scale terrain forcing. We illustrate these effects with observations from a mesoscale wind network for several cases, and use the model to show the relationship between the local winds, the prevailing synoptic conditions, and regional and local topographical features.

Corresponding author address: Dr. J. Christopher Doran, Battelle/Pacific Northwest Laboratories, P.O. Box 999, Richland, WA 99352.

2. Site

The local study area is the U.S. Department of Energy's Hanford site in south-central Washington, and is located along the western edge of the Columbia Basin. It is bordered by gradually rising terrain toward the east and much more complicated mountain and valley terrain to the north, west, and southwest. Figure 1a shows the topography of the Pacific Northwest used in our numerical simulations (described in section 4), and the location of the Hanford site relative to some of the principal features of the region. There are major gaps through the Cascade Mountains to the south, in the Columbia Gorge, and to the north, over Snoqualmie Pass and through the Kittitas Valley. Figure 1b shows additional details of the topography of the Hanford site and the surrounding area. The local terrain is dominated by Rattlesnake Ridge, which runs roughly northwest to southeast; other significant features include the Yakima River valley to the west, the Horse Heaven Hills to the south, and the Saddle Mountains to the north.

Data collected on the site include hourly temperatures and wind speeds from 23 surface telemetry stations, wind and temperature data from a 122-m tower (marked HMS on the map), and twice-daily pibal soundings.

3. Observations

We have chosen two cases to illustrate the wind-field characteristics that are frequently observed during wintertime transition periods, that is, periods between high pressure ridge and strong westerly synoptic patterns. The cases represent a primary flow pattern over the Hanford region identified by a principal-component analysis applied to the horizontal wind components (Skyllingstad and Schwartz 1989). For the Hanford site, the method yields the first principal-component wind field, shown in Fig. 2. The pattern features moderate southwesterly winds in the southern part of the Hanford site, and light and variable winds in the northern part. This flow pattern is found primarily in the winter, which suggests that its establishment and evolution are related to the existence of persistent surface inversions over the area.

Our first case, on 1 January 1990, followed a weak cold-frontal passage, and was marked by low-level winds predominantly from the west. The surface pressure field over the state of Washington showed a ridge of high pressure to the south with an increasing gradient toward the north. Westerly winds of 15 m s^{-1} between the surface and 2000 m were measured by a rawinsonde at Spokane (approximately 200 km to the northwest) at 0400 PST. At HMS, pibal observations at 1200 PST showed a generally westerly flow of 6–7 m s^{-1} up to about 1200 m, where the winds backed to a southwest direction. The atmosphere was weakly stable, with a nearly isothermal profile at the 122-m tower.

At 0900 PST, the winds from the Hanford telemetry network clearly showed the influence of the local terrain (Fig. 3a). In the south, moderately strong southwest winds were observed, with flow out of the Yakima Valley and from across the Horse Heaven Hills. Farther north, where the flow was blocked by Rattlesnake Ridge, the winds decreased, becoming light and variable near the northern edge of the site. Three hours later, around the time of the pibal release, the winds over the north portion of the site had switched to the northwest while southwesterly winds continued in the south (Fig. 3b). The combination of these two flows produced a region of strong horizontal wind shear over the site. Although this pattern is similar to that found in a frontal zone, temperatures over the area were relatively uniform, and analysis at a later time (i.e., 2200 PST) showed nearly the same winds and temperatures.

The second case, 1 February 1990, took place prior to the passage of a cold front. The Spokane rawinsonde sounding again showed winds of approximately 15 m s^{-1}, but the directions were shifted to the south by 20°–30°. The HMS pibal winds had more low-level directional shear than in the first case, backing from roughly 285° at the surface to 245° at 1000 m. Winds near the surface were less than 3 m s^{-1} and increased to over 8 m s^{-1} above 1000 m. The turning of the wind below 700 m was strongly influenced by the elevated terrain of Rattlesnake Ridge to the west, and is therefore not considered representative of the larger-scale wind direction. A plot of the surface telemetry network wind data again shows the effect of the terrain on the surface wind field (Fig. 4a). As in the first case, there was moderately strong southwest flow over the southern part of the site. The decrease in wind speeds in the north was even more pronounced than before, and a corresponding temperature difference over the area was also noted, with the nearly calm stations in the northern sections being as much as 5 K colder than stations in the southern sections. At HMS, an inversion persisted throughout the day, with temperatures at the 122-m level averaging nearly 4 K higher than those at the 1-m level during the morning hours after sunrise. In contrast to the previous case, northwest flow failed to develop over the north part of the site (Fig. 4b).

The two cases presented here are consistent with the principal-component wind-field pattern displayed in Fig. 2, with each case showing southwesterly flow in the south and a horizontal shear zone crossing the site. However, the cases are distinct with regard to the evolution of the wind direction in the north part of the site. For both cases there is an apparent blockage of flow by Rattlesnake Ridge during the morning hours, resulting in a nearly calm zone in the north. When the winds aloft (i.e., above the level of Rattlesnake Ridge) were from the west-southwest (case 1), a surface flow

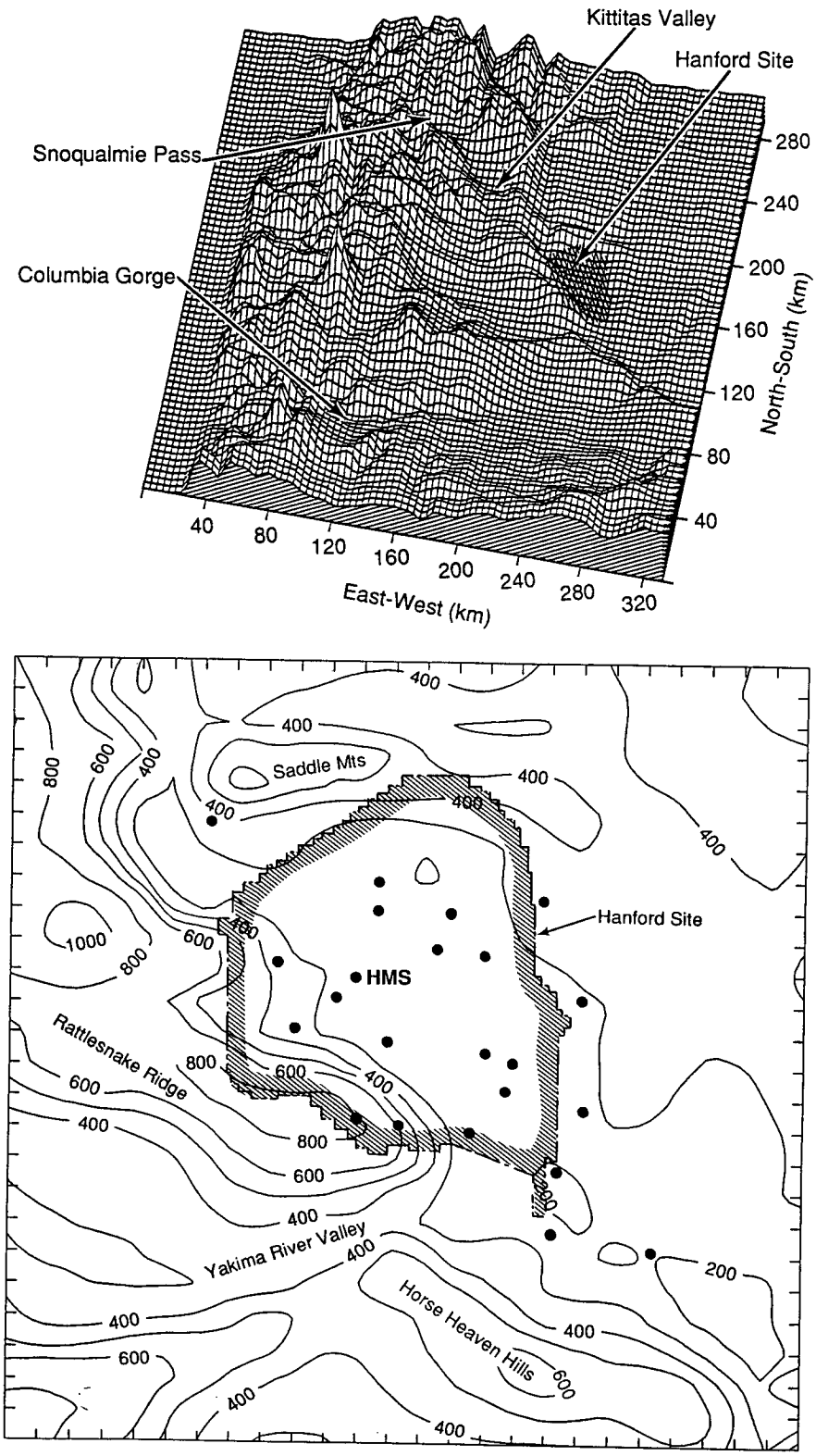

FIG. 1. (a) Pacific Northwest topography used for numerical simulations. (b) Contour map of the Hanford site and surrounding area. Dots mark positions of surface telemetry stations; HMS is location of 122-m tower. Contour intervals are in meters, and tick marks are 4 km apart.

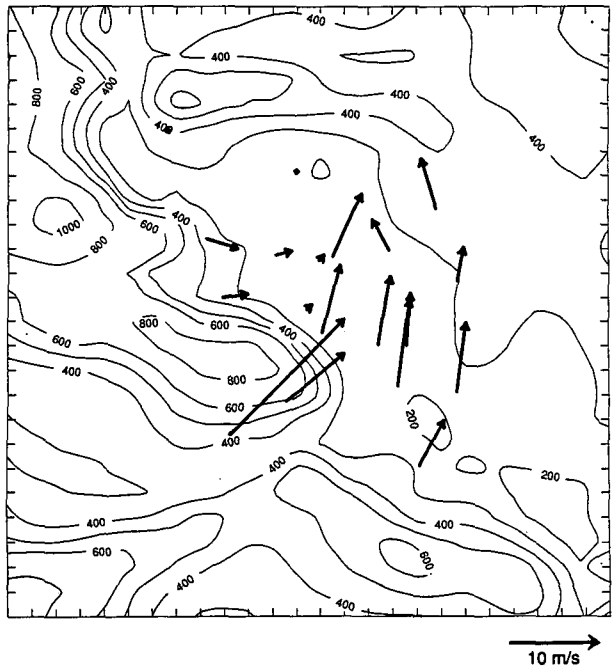

FIG. 2. First principal-component wind field for Hanford area.

from the northwest subsequently formed. When the winds aloft were shifted somewhat more to the southwest (case 2), the winds to the north remained nearly calm and the region of southwest surface flow extended farther northward.

4. Numerical model simulations

A hydrostatic numerical mesoscale model was used to identify the factors responsible for the evolution of each of the two different wind regimes, that is, the development of a northwest flow or the maintenance and northward propagation of southwest flow in the northern part of the Hanford site. We were also interested in possible implications for forecasting and the use of mesoscale models in complex terrain. The model was adapted from one developed by Pielke (e.g., Mahrer and Pielke 1977; McNider and Pielke 1984). The code was modified to incorporate a turbulent exchange scheme based on the prognostic turbulent kinetic energy formulation of Mellor and Yamada (1982). Turbulence second moments describing vertical transport of heat and momentum are found from a set of diagnostic equations; these equations are given in Yamada (1983) and constitute a slight simplification of his level 2.5 scheme. The turbulent mixing length was also found using a diagnostic equation (Mellor and Yamada 1982; Doran et al. 1990).

Calculations were done on an 84 × 74 grid, with 4-km grid spacing, which produced a domain large enough to extend west of the Cascade Mountains (Fig. 1). Additional elevated terrain lies still farther to the west on the Olympic peninsula, but its effects were assumed to be unimportant for this study. A horizontally homogeneous surface with a uniform roughness length of 0.1 m was chosen for the entire domain; although this represents a simplification of the actual surface characteristics, tests indicate that the general

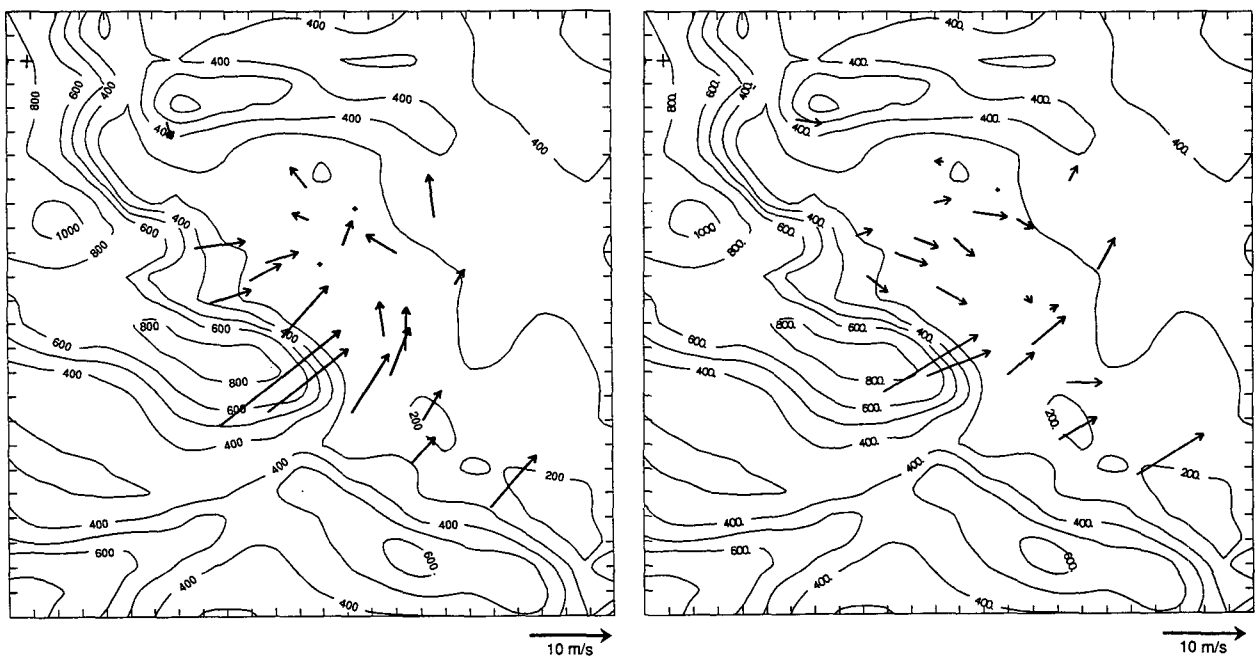

FIG. 3. Observed surface wind field on 1 January 1990. (a) 0900 PST and (b) 1200 PST.

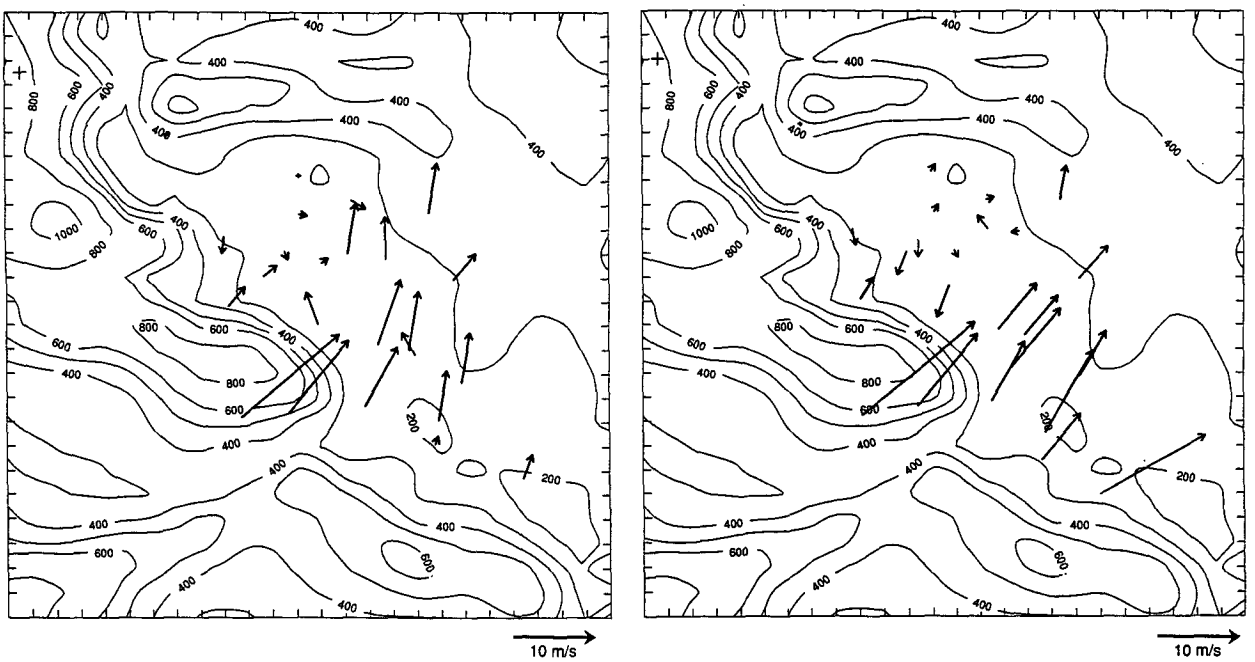

FIG. 4. Observed surface wind field on 1 February 1990. (a) 0900 PST and (b) 1200 PST.

results should not be significantly affected by this approximation. There were 20 grid points in the vertical, ranging from a grid spacing of 10 m at the lowest level to 2000 m at the top of the model at 12 000 m. Turbulent fluxes at the lowest grid level were determined from similarity formulas (Businger 1973). A sponge layer was used to reduce wave reflections at the top (Klemp and Lilly 1978). A horizontally stretched grid and zero-gradient boundary conditions were applied at all lateral boundaries.

For each simulation, a geostrophic wind profile was defined. A one-dimensional model was run to establish an initial profile, which was then interpolated to grid points above the elevated terrain. The full three-dimensional model was run for 3 h without surface heating or cooling to allow the wind and temperature fields to approach equilibrium. Surface cooling then proceeded for three more hours, using a surface energy balance scheme described by Yamada (1981), until sunrise around 0730 PST. After sunrise, solar heating appropriate for mid-January conditions in the Pacific Northwest was used to warm the surface until 1500 PST. At 0700 PST, the temperature over a grid point representing the area around HMS showed a near-surface inversion of approximately 4.5 K in the first 100 m.

The initial temperature profile and the variation of wind speed with height were fixed for most of our experiments, while the wind direction was varied. Our intent was to examine generic factors that governed the observed flow patterns rather than to simulate a particular case. During transition periods from high pressure ridge to trough patterns, upper-level winds often increase while lower-level pressure gradients remain small. Accordingly, we chose a geostrophic wind whose speed increased linearly from 3 m s^{-1} at the surface to 15 m s^{-1} at 2200 m; above this height the wind speed remained constant at 15 m s^{-1}. Thermal wind balance then requires that the equation for potential temperature be modified to include a term describing the advection of the mean state potential temperature (e.g., Lee et al. 1989). In practice, this contribution proved to be of little importance to our results. The direction of the geostrophic wind was constant with height and varied from 215° to 275° for the various experiments.

The resultant wind fields were examined to determine their sensitivity to the ambient wind directions. Figure 5 shows the near-surface (10 m AGL) winds at 1300 PST for ambient wind directions of 255° and 225°. The patterns are similar to those discussed earlier for the cases shown in Figs. 4a and 4b. In the 225° case, there is a moderate southwesterly flow in the southern part of the Hanford site but the winds to the east of Rattlesnake Ridge are much lighter. For the 255° case, there are again stronger winds to the south, but farther north the winds are nearly calm. Near the northern edge of the domain, the winds are from the northwest.

The mechanism that produces northwest winds in the 255° case can be seen by examining the wind fields over the full modeling domain. Figure 6a shows the near-surface winds for 1300 PST. Air passing over and through the gaps in the Cascades mountain barrier is deflected toward the southeast by the higher terrain to the north. In particular, air traveling east in the Sno-

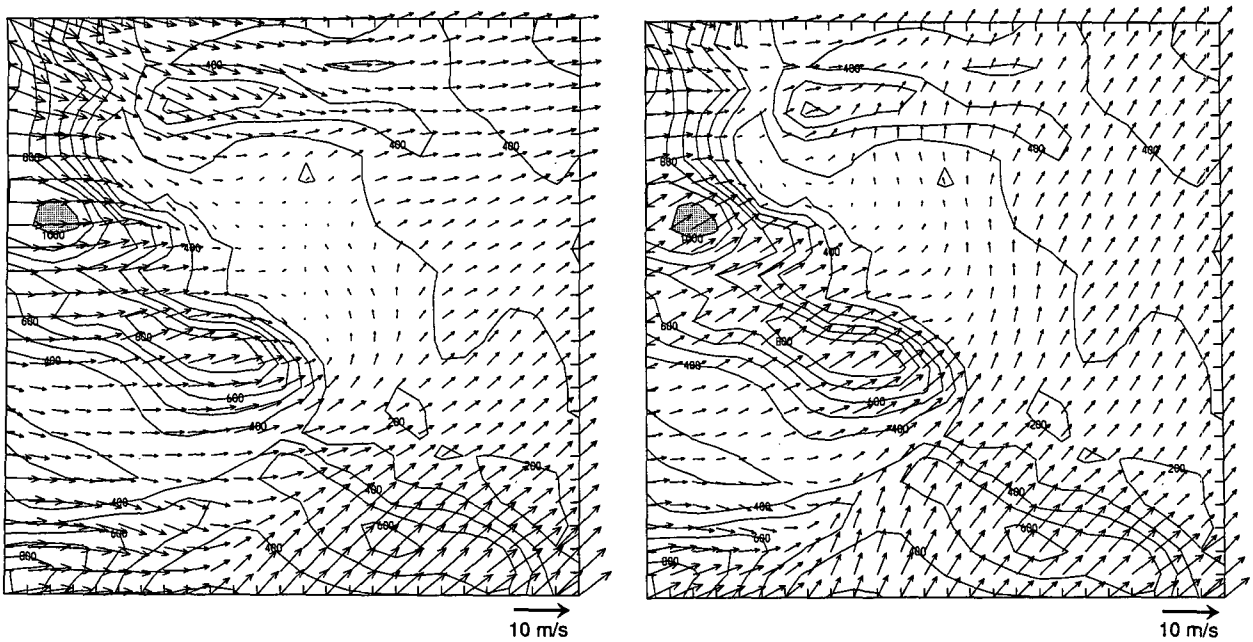

FIG. 5. Simulated surface winds near Hanford area at 1300 PST. (a) Ambient winds from 255°, (b) ambient winds from 225°. Tick marks are 4 km apart. Stippled areas mark regions with elevations over 1000 m.

qualmie Pass area is deflected toward the south and continues toward the northern portions of the Hanford site. These winds decrease as they approach the site itself, and over the northern portions of the site the winds are nearly calm. Near HMS, the winds below 100 m are less than 1 m s^{-1}, and out of the west. Two hours later, northwest winds are also found in the northern part of the Hanford site (Fig. 6b) and the pattern is similar to the observations presented earlier in Fig. 4b. Over HMS, northwest winds are found

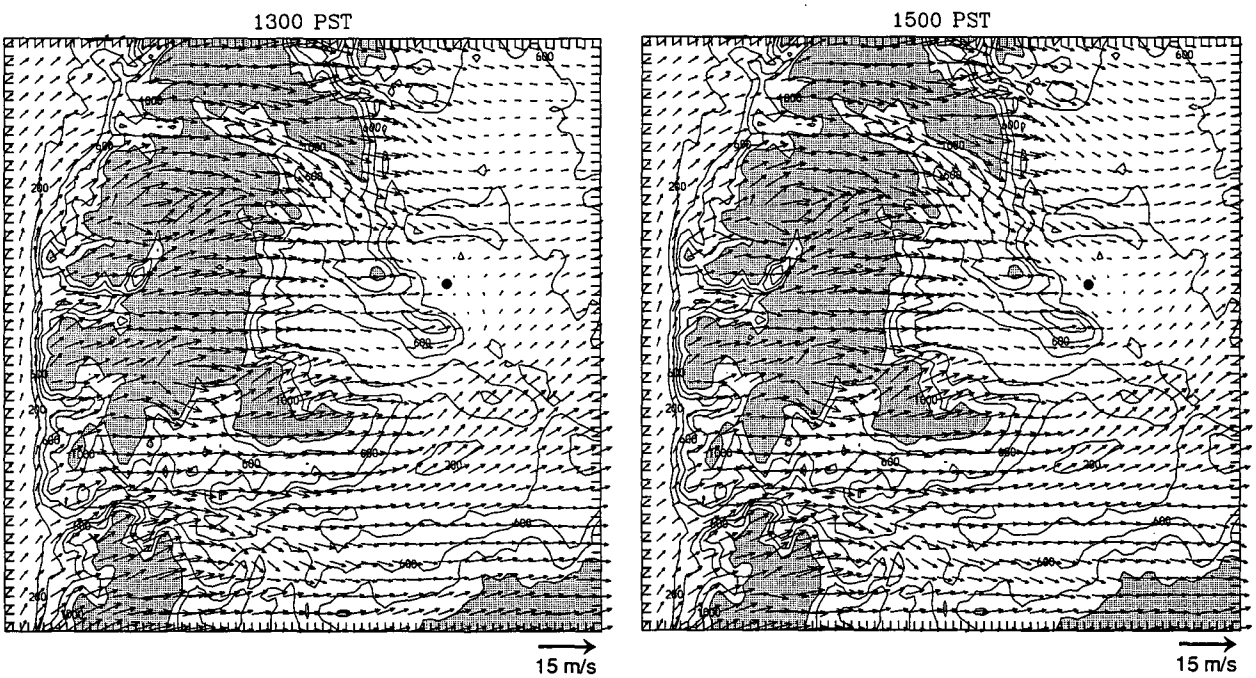

FIG. 6. Simulated surface winds over Pacific Northwest for ambient winds from 255°. (a) 1300 PST, (b) 1500 PST. Tick marks are 4 km apart. Stippled areas mark regions with elevations over 1000 m; dot near right center of figure marks location of HMS.

through a depth of 400 m, and wind speeds near the surface are over 2 m s^{-1}. The development of these northwest winds appears to be caused by a combination of two factors. The first is the propagation of northwest flow to the southeast by advection, that is, from the $u_j \partial u_i / \partial x_j$ term in the momentum equation. The second is the turbulent transport of faster moving air toward the surface through a well-mixed layer. Figure 7 shows such a layer east of Rattlesnake Ridge, where northwest winds have developed at the surface. Farther to the east, where surface winds are still nearly calm, a colder pocket of air remains. The increases in the northerly wind components over the northeast parts of the modeling domain are comparable in magnitude to those expected from the Coriolis acceleration arising from the corresponding increases in the westerly components. The latter effect is especially apparent north of the Hanford site, where westerly flow descending from the higher elevations turns toward the south over the flatter terrain.

In the south, as the higher terrain north of the Columbia Gorge slopes down to the east, the winds flowing east through the gorge turn back toward the northeast again, driven by the synoptic pressure gradient. This flow, coupled with the blocking effect of the southern edge of Rattlesnake Ridge, produces the southwest flow in the southern portion of the Hanford site and a weak horizontal vortex in the lee of Rattlesnake Ridge. A horizontal shear zone is situated over the site, marking the transition between the northwest winds to the north and the southwest winds to the south. For more northerly ambient winds, this zone moves still farther to the south. For more southerly winds, the zone moves to the north until it disappears altogether for ambient wind directions around 215°.

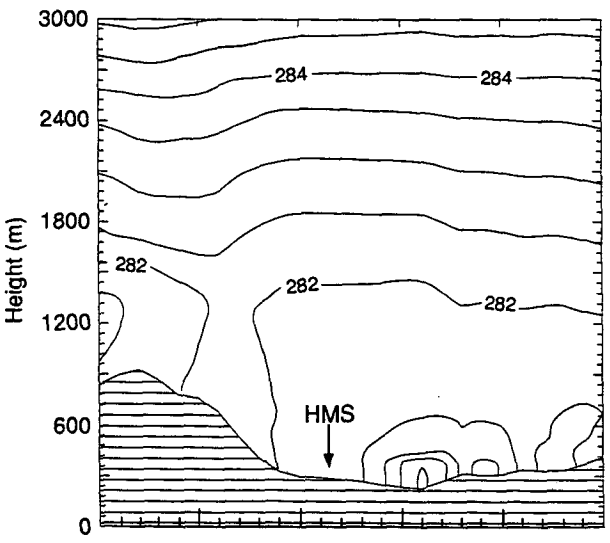

FIG. 7. East–west cross section through HMS, showing contour lines of potential temperature. Contour interval is 0.5 K.

Figure 8 shows simulated wind speed and direction profiles near HMS for the two cases at 1500 PST. The sensitivity of the near-surface winds to changes in the upper-level winds is apparent.

These wind patterns are in good qualitative agreement with observations, and illustrate the importance of both local and regional topography in determining the local flow characteristics. One difference between the model results and the observations from the 1 February 1990 case discussed earlier is that the model failed to produce the strong temperature gradient observed between the northern and southern portions of the site. The measured winds in the north were nearly calm throughout the day, enabling a low-level inversion to be maintained there. The model does not produce a sufficiently sharp transition between the two flow regimes, that is, the southwest winds in the south and calm conditions in the north, and instead generates enough mixing to break the surface inversion throughout most of the domain. The more gradual transition in flow-field characteristics produced by the model is probably related to the smoothing of the temperature fields, but apparently does not have a serious impact on other features of the wind field.

We carried out another experiment in which the geostrophic wind direction was again 255° but the wind speed increased to 20 m s^{-1} at 2200 m instead of 15 m s^{-1}, as in the previous cases. This relatively small increase in shear results in significantly greater vertical mixing of air over the Hanford site. As a result, by 1300 PST the winds over the site are generally westerly even though the low-level flows through the gaps in the Cascades are still from the northwest. Moreover, the inversion to the lee of Rattlesnake Ridge is weaker, the nearly stagnant area disappears, and the horizontal shear zone that characterized the earlier 255° simulation is also absent. In this case, flows over the Hanford site depend more strongly on synoptic wind conditions and less on either local or regional topographic features.

Thus, the importance of shear in removing cold air differs markedly from the cases discussed by Lee et al. (1989), who used a two-dimensional simulation to study the effects of cold air trapping in the lee of a 2-km mountain with a 20-km half-width. In contrast to our simulations, their cases had a low-level zone of winds that blew counter to the prevailing flow, trapping cold air against the mountain. In addition, the two-dimensional nature of their topography precluded the types of channeling and deflection of flows through mountain gaps that are seen in our results.

We carried out two additional experiments to assess the importance of thermal stratification on the local wind-flow patterns. In the first experiment, a 255° geostrophic wind was again specified, but solar heating was not turned on. At 1500 LST, the winds in the lee of Rattlesnake Ridge and in the Yakima Valley remained nearly calm, and the horizontal shear zone over the Hanford site was absent. The southwest winds in

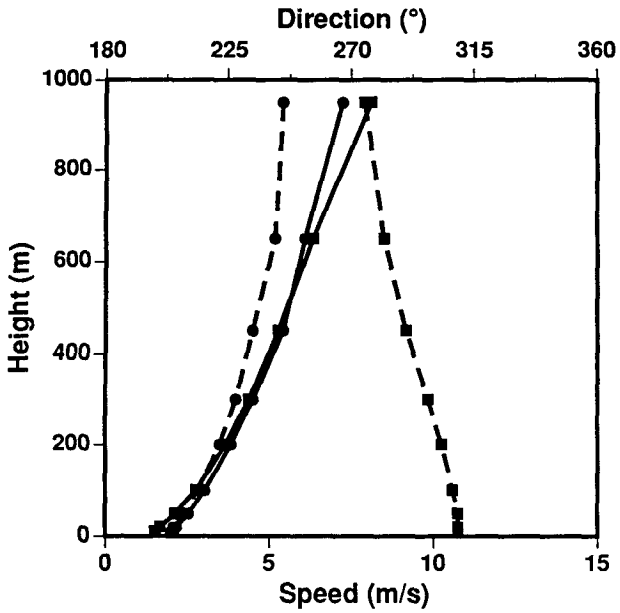

FIG. 8. Simulated wind speed (solid lines) and direction (dashed lines) profiles near HMS at 1500 PST for ambient winds at 225° (circles) and 255° (squares).

the southern end of the site were much weaker than in the case with solar heating, and northwest winds failed to develop in the northern areas of the site. For our second experiment on stability effects, we assumed a mid-April date for the simulation so that the solar insolation was considerably stronger than for the mid-January cases. All other conditions were the same as for our basic 255° simulation. As expected, the stronger heating resulted in more vigorous vertical mixing in the lee of Rattlesnake Ridge. By 1500 PST, northwest flow had developed over most of the site with westerly flow near the southern boundary, but there was no evidence of the horizontal shear zone seen in the mid-January simulation. These results show that if an inversion is too strong, the horizontal shear zone over the site will not develop and local terrain blocking is the major factor in determining local flow patterns. If the inversion is too weak, blocking is ineffective, the shear zone will again be absent, and synoptic winds become the major factor. For intermediate values of inversion strength, a horizontal shear zone will develop and the flow patterns are determined by a combination of synoptic forcing and regional- and local-scale topographic effects.

5. Discussion and summary

There are a number of interesting implications from this study for applications of mesoscale models to regions of complex terrain. It is clear that under some circumstances a proper simulation of the flows may require incorporation of terrain features several hundred kilometers upwind, while under other conditions the local topography may dominate. The use of extended modeling domains is then required even if the concern is with more localized wind and temperature fields. Nesting of models has found increasing favor as a means of maintaining high resolution in one or more areas of interest while allowing the use of extended domains to include larger-scale features; simply reducing the model resolution to make the model more economical to run is not a satisfactory approach. In one experiment in which we doubled the grid spacing to 8 km, many of the larger-scale flow features were retained but the flow pattern in the lee of Rattlesnake Ridge was not reproduced. When the resolution was decreased still further, to 16 km, the deflection of the winds in the Snoqualmie Pass area disappeared. Thus, even nesting may be ineffectual for the cases considered here; a nesting ratio of 4:1 in grid resolution could miss a significant feature of the larger-scale flows. A large outer domain is required, but its resolution clearly cannot be too coarse, and it is difficult to specify, a priori, what resolution is required for a particular application.

The simulations also indicate one of the difficulties of operational wind forecasting in regions like our study area. At some points in the model domain, a shift in synoptic wind direction of only 30° results in a difference of nearly 100° in wind direction in the lowest 200 m. Such sensitivity to small changes in the synoptic forcing could have important implications for air pollution or emergency response applications in areas with similar characteristics. At Hanford, some information on the winds aloft is obtained from observations collected on top of Rattlesnake Ridge. An alternative approach would be to use remote-sensing wind profilers to obtain data on the structure of the boundary layer, but care must be exercised in the profilers' placement and use. For example, wind speed and direction profiles at 1300 PST were obtained from the simulations for the 225° and 255° cases at a point just to the southwest of Rattlesnake Ridge. In the lowest 400 m, the profiles are quite similar. At higher elevations the differences in wind direction become more apparent, but do little to suggest the significant changes that occur in wind fields two hours later near HMS, only 40 km to the northeast. Wind speed and direction profiles computed over HMS at 1300 PST are not much more instructive. There is a nearly calm region in the first 100 m above the surface for both cases so that, in practice, local terrain effects not resolved in the model would probably determine the observed wind directions under such conditions. Above 100 m, wind speeds increase somewhat but differences in direction for the two cases average less than 30°. These differences, too, are a poor predictor of the magnitude of the subsequent differences in the near-surface wind behavior 2 h later. A study combining the use of profiler-derived wind data, wind-field analyses, and mesoscale modeling to assist

in the interpretation of the results could prove quite useful in improving forecast accuracy.

Other wind patterns observed over the Hanford site may also show dependencies on both large- and small-scale terrain forcing. During the late spring and summer months, flows driven by the temperature differences between the Cascades and the Columbia Basin frequently occur around sunset and persist for several hours over the northern portions of the Hanford site. The strength, timing, and extent of these flows are no doubt dependent upon factors similar to those discussed above, and will be the subject of a future analysis.

In summary, our study has shown the following:

1) During the winter and in the presence of an inversion, flows over the Hanford site are often dominated by local terrain effects. A horizontal shear zone forms in the lee of Rattlesnake Ridge, and the development of this zone shows little sensitivity to variations in synoptic wind direction.

2) As the thermal stratification weakens, winds in the northern areas of the site evolve in a manner that is highly sensitive to the synoptic winds. Moreover, for some synoptic wind directions, the local winds are forced, in part, by the large-scale topographical features of the Cascade Mountains.

3) In the presence of stronger vertical wind shear, the synoptic-scale winds dominate and the importance of local- and regional-scale topographical features diminishes.

4) The results illustrate some of the difficulties associated with the use of mesoscale models in regions of complex terrain. Limited domain models may eliminate distant but significant terrain features, and nested models may fail to resolve important flow patterns in regions of coarser resolution.

Acknowledgments. This work was supported by the U.S. Department of Energy (DOE) under Contract DE-AC06-76RLO 1830. The study was carried out under the auspices of the Atmospheric Studies in Complex Terrain (ASCOT) program and the Meteorological and Climatological Assessment program at Pacific Northwest Laboratory. Pacific Northwest Laboratory is operated for DOE by Battelle Memorial Institute.

REFERENCES

Businger, J. A., 1973: Turbulent transfer in the atmospheric surface layer. *Workshop on Micrometeorology,* Boston, Amer. Meteor. Soc., 392 pp.

Doran, J. C., T. W. Horst, and C. D. Whiteman, 1990: The development and structure of nocturnal slope winds in a simple valley. *Bound.-Layer Meteor.,* **52,** 41–68.

Durran, D. R., 1990: Mountain waves and downslope winds. *Atmospheric Processes over Complex Terrain,* W. Blumen, Ed., Amer. Meteor. Soc., 59–81.

Klemp, J. B., and D. K. Lilly, 1978: Numerical simulation of hydrostatic mountain waves. *J. Atmos. Sci.,* **35,** 78–107.

Lee, T. J., R. A. Pielke, R. C. Kessler, and J. Weaver, 1989: Influence of cold pools downstream of mountain barriers on downslope winds and flushing. *Mon. Wea. Rev.,* **117,** 2041–2058.

Mahrer, Y., and R. A. Pielke, 1977: A numerical study of the air flow over complex terrain. *Contrib. Atmos. Phys.,* **50,** 98–113.

McNider, R. T., and R. A. Pielke, 1984: Numerical simulation of slope and mountain flows. *J. Climate Appl. Meteor.,* **23,** 1441–1453.

Mellor, G. L., and T. Yamada, 1982: Development of a turbulence closure model for geophysical fluid properties. *Rev. Geophys. Space Phys.,* **20,** 851–875.

Skyllingstad, E. D., and M. N. Schwartz, 1989: The identification of terrain-induced circulations using principal components. Preprints, *11th Conf. on Probability and Statistics in Atmospheric Sciences,* Boston, Amer. Meteor. Soc., 292–296.

Yamada, T., 1981: A numerical simulation of nocturnal drainage flow. *J. Meteor. Soc. Japan,* **59,** 108–122.

——, 1983: Simulations of nocturnal drainage flows by a q^2–l turbulence closure model. *J. Atmos. Sci.,* **40,** 91–106.